

Gaussianizing the non-Gaussian lensing convergence field II: the applicability to noisy data

Yu Yu,^{1,*} Pengjie Zhang, Weipeng Lin, Weiguang Cui,¹ and James N. Fry²

¹*Key laboratory for research in galaxies and cosmology, Shanghai Astronomical Observatory, Chinese Academy of Science, 80 Nandan Road, Shanghai, China, 200030*

²*Department of Physics, University of Florida, Gainesville FL 32611-8440, USA*

In paper I (Yu et al. 2011 [1]), we show through N-body simulation that a local monotonic Gaussian transformation can significantly reduce non-Gaussianity in noise-free lensing convergence field. This makes the Gaussianization a promising theoretical tool to understand high-order lensing statistics. Here we present a study of its applicability in lensing data analysis, in particular when shape measurement noise is presented in lensing convergence maps. (1) We find that shape measurement noise significantly degrades the Gaussianization performance and the degradation increases for shallower surveys. (2) Wiener filter is efficient to reduce the impact of shape measurement noise. The Gaussianization of the Wiener filtered lensing maps is able to suppress skewness, kurtosis, 5th- and 6th-order cumulants by a factor of 10 or more. It also works efficiently to reduce the bispectrum well to zero.

PACS numbers: 98.80.-k; 98.65.Dx; 98.62.Ve; 98.62.Sb

I. INTRODUCTION

Weak gravitational lensing, a powerful probe of the dark universe, is facing many challenges. One of them is the nonlinear evolution of the large scale structure (LSS). The non-Gaussianity induced by the nonlinear evolution pushes the cosmological information into high-order statistics, leading to the loss of constraining power from the 2-point statistics (the power spectra and equivalently the correlation functions) alone. Recently several works focus on nonlinear local transformation of the 2D lensing and 3D matter and galaxy fields to reduce the non-Gaussianity [1–7]. This procedure is shown to be promising. The nonlinear transformation changes the information distribution in the hierarchical statistics. It makes the cosmic fields close to Gaussian and hence significantly improves the information we can extract from low-order statistics.

Most of these works adopt the logarithmic transformation. Instead we choose a Gaussian transformation, which is defined as a local monotonic transformation to Gaussianize the one-point PDF [1]. Throughout the paper we call the applying of this transformation as *the Gaussianization*. This approach is motivated by the Gaussian copula hypothesis [8]. If this hypothesis is valid, the Gaussianization will make all the statistics Gaussian, besides the one-point PDF.

Through N-body simulations, we quantified the performance of the Gaussianization on 2D lensing field against various measures of non-Gaussianity, such as skewness, kurtosis, fifth- and sixth-order cumulants as functions of smoothing radius, and the bispectrum. We found that the Gaussianization works surprisingly well. It suppresses the above non-Gaussianity measures by orders of

magnitude and effectively reduce them to zero. This implies that in many exercises we can treat the new field as Gaussian. The Gaussianization procedure then transports cosmological information in higher-order statistics of the original lensing fields into the power spectrum of the new one. For this reason, theoretical modeling of the weak lensing statistics can be significantly simplified.

However, this does not necessarily mean that the Gaussianization procedure works for real data, in which there are various measurement noises. A prominent one is the shape measurement noise from the random galaxy shapes. Its impact on the Gaussianization can be figured out straightforwardly in two limits. (1) When the shape noise is negligible with respect to the lensing signal, the Gaussianization works pretty well, as shown in paper I. (2) When the shape noise overwhelms the lensing signal, the Gaussianization collapses. Let's look at the case of sufficiently large pixel with $N \gg 1$ galaxies. Due to the central limit theorem, the shape noise distribution approaches to Gaussian, so does the one-point PDF. Hence the Gaussianization transformation becomes trivial and the Gaussianization fails.

Hence whether or not the Gaussianization is applicable to lensing surveys is a nontrivial question. To investigate the applicability, we add shape measurement noise to the simulated lensing convergence maps. Following paper I, we then test the performance of the Gaussianization through several measures of non-Gaussianity, including the cumulants up to 6th-order of the smoothed field,

We find that the performance of the Gaussianization is strongly affected by the shape measurement noise. However, if we Wiener filter the lensing maps first and then perform the Gaussianization, it can still work pretty well for DES-like or LSST-like surveys.

Our paper is organized as follows: In §II we briefly introduce the way to construct noisy weak lensing convergence fields using N-body simulation. Measures of the non-Gaussianity, i.e. the measures of the Gaussianization

*Electronic address: yuyu22@shao.ac.cn

performance in noisy case are presented in §III. To reduce the degradation of the Gaussianization method cause by shape measurement noise, we propose Wiener filter as a remedy and redo the analysis in §IV. In §V we summarize the results and outline the key issues for further investigation.

II. SIMULATED LENSING CONVERGENCE MAPS WITH SHAPE MEASUREMENT NOISE

We refer the readers to paper I (Yu et al. 2011 [1]) and the references therein for the weak lensing basics. In the first step, we construct noise-free lensing convergence maps same as paper I. Our N-body simulations were run using the Gadget-2 code [9] adopting the standard Λ CDM cosmology, with $\Omega_m = 0.266$, $\Omega_\Lambda = 1 - \Omega_m$, $\sigma_8 = 0.801$, $h = 0.71$ and $n_s = 0.963$. The output redshifts are specified such that any two adjacent outputs are separated by the box size $L = 300h^{-1}\text{Mpc}$ in comoving distance. More details can be found in [10]. We stack eight randomly shifted and rotated snapshots to comoving distance $2400h^{-1}\text{Mpc}$ to make κ maps. These lensing maps correspond to source redshift $z \approx 1.02$, with map size being $7.64^\circ \times 7.64^\circ$. When analyze these maps, we use 512^2 uniform grids, corresponding to pixel size of $0.9'$. The Gaussianization transformation is nonlinear and its dependence on pixel size is nontrivial. We leave this issue for future work.

In observation, for the lensing convergence map reconstructed from cosmic shear, the measurement noise can be approximated as a Gaussian random noise, with a rms of $\sigma_N = 0.2/\sqrt{N}$, where N is the mean number of galaxies per pixel. We add two levels of noise into the convergence maps constructed from simulation to test the Gaussianization method. The two levels of noise correspond to source galaxy number density of $10/\text{arcmin}^2$ and $40/\text{arcmin}^2$. Hereafter we denote the two cases as case A and case B. The first corresponds to a DES [14] like survey and the second corresponds to a LSST [15] like survey. In reality, these surveys not only have different source galaxy number density, but also have different source galaxy redshift distribution and hence have different lensing signal. Since our purpose is to investigate the dependence of Gaussianization on measurement noise, we neglect the difference in source redshift distribution and fix the lensing signal, but vary the measurement noise. For each noise level, we produce 20 Gaussian white noise maps and add them into convergence maps pixel by pixel. Throughout the paper, we denote the true lensing signal as κ_T , the noise as κ_N and the sum as $\kappa \equiv \kappa_T + \kappa_N$.

For the given pixel size, the corresponding noise rms is ~ 0.07 for case A and ~ 0.035 for case B. The lensing signal rms is about 0.02. Hence for both cases, noise dominates over the signal and hence significantly changes the one-point PDF and push it approaching a Gaussian form. The numerical results of one convergence map with two levels of noise added are presented in the left column

of Fig.1. Indeed, for case A, there is almost no visible deviation in the one-point PDF from the Gaussian distribution. For case B, only small deviations can be seen.

III. GAUSSIANIZATION PERFORMANCE ON NOISY MAPS

Here we briefly introduce the Gaussianization we use. Details are given in paper I. The Gaussian transformation $\kappa \rightarrow y$ is defined as follow:

$$\int_{-\infty}^y P_G(y)dy = \int_{-\infty}^{\kappa} P(\kappa)d\kappa, \quad (1)$$

with normalization at zero point:

$$\left. \frac{dy}{d\kappa} \right|_{\kappa=0} = 1. \quad (2)$$

Here by definition $P_G(y) = \exp(-y^2/2\sigma_y^2)/\sqrt{2\pi}\sigma_y$ is the Gaussian PDF and σ_y is the rms dispersion of y . We obtain this transformation numerically for each pixelized simulated map.

By definition, the one-point PDF of the y field of the given pixel size is Gaussian. However, this does not necessarily mean that the resulting field y is a multivariate Gaussian random field. For example, if we smooth the field, the one-point PDF of the smoothed field y_S can be non-Gaussian. Following paper I, we will evaluate various non-Gaussianity statistics, such as the cumulants as a function of smoothing scale and the bispectrum. The reduced cumulants K_n ($n = 1, 2, \dots$) is defined by

$$K_n \equiv \frac{\langle y_S^n \rangle C}{\langle y_S^2 \rangle^{n/2}}. \quad (3)$$

The reduced bispectrum

$$q(\vec{\ell}_1, \vec{\ell}_2, \vec{\ell}_3) = \frac{B(\vec{\ell}_1, \vec{\ell}_2, \vec{\ell}_3)}{[P(\ell_1)P(\ell_2) + \text{cyc.}]^{3/4}}, \quad (4)$$

with $\vec{\ell}_1 + \vec{\ell}_2 + \vec{\ell}_3 = 0$. We express q in the coordinate (l, u, α) , where $l \equiv l_1$, $u \equiv l_2/l_1$ and $\alpha = \arccos(\vec{l}_1 \cdot \vec{l}_2)/l_1 l_2$.

Again, we caution the readers that the definitions of the cumulants and reduced bispectrum are different from the widely used definitions in large scale structure study. They are designed to be invariant under the transformation $y \rightarrow Ay$ where A is an arbitrary constant. This property is desirable when comparing these non-Gaussianity measures before and after the Gaussianization.

A. The κ - y relation of noisy maps

The Gaussian transformations we obtain are presented in the left panel of Fig.2. For case A, noise dominates over

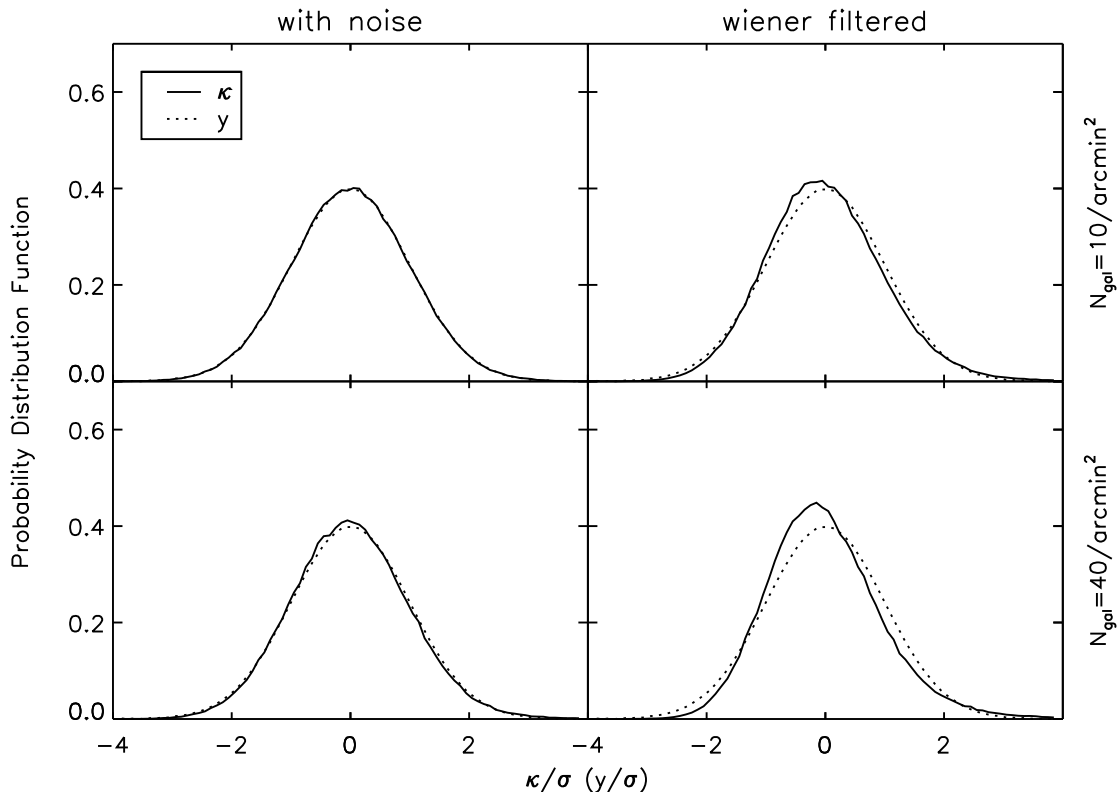


FIG. 1: The left column shows the PDFs of one convergence map we constructed with two levels of noise added. The right column shows the PDFs of the convergence map with noise reduction by the Wiener filter. The PDFs of the field after the Gaussianization is also plotted in dotted line, which is just standard Gaussian distribution by definition. From the PDF we can see that the two levels of Gaussian noise both dominate the distribution. After the Wiener filter applied, the non-Gaussianity is recovered to some extent.

signal ($|\kappa_N| \geq |\kappa_T|$) for almost all of the pixels. Since the noise PDF is Gaussian, to a good approximation, we have $y = \kappa$. This is what we see from Fig. 2. On the other hand, visible deviation from $y = \kappa$ can be found at the end of high κ , where the lensing signal can dominate over the noise due to its skewed PDF.

For case B, noise is reduced by a factor of 2, so the non-Gaussianity of the PDF is less affected. As a consequence, we find larger deviation from $y = \kappa$.

The Gaussian transformations for 20 realizations converge with each other very well. The convergence is much better than what found in previous work where the lensing maps are free of noise. This better convergence is also a manifestation of overwhelming shape measurement noise.

B. The cumulants of smoothed noisy maps

The cumulants K_n of the smoothed field y_S are non-trivial checks of non-Gaussianity, despite the fact that the cumulants of the unsmoothed y field are Gaussian by definition. Smoothing introduces pixel-pixel correlation and gives rise to non-Gaussian y_S cumulants. The results for

the cumulants of the smoothed field up to the sixth-order are presented in the left column of Fig.3 & 4 for case A and Fig.5 & 6 for case B. The same as paper I, all results are averaged over 20 realizations and the error bars are the dispersions between these realizations. To highlight the performance of Gaussianization, $K_n(y_S)/K_n(\kappa_S)$ as a function of smoothing scale is shown in Fig.7.

Contaminations of shape measurement noise significantly changes the behavior of the cumulants. (1) since the noise field is Gaussian and the measurement noise often dominates the lensing signal, the cumulants $K_n(\kappa_S)$ are much lower than the corresponding ones in the noise-free case (paper I). (2) Smoothing suppresses the noise more efficiently than the signal, since the power of noise is more concentrated to small scales (e.g. zero-lag). Hence for sufficiently large smoothing scale, signal can dominate over noise and the non-Gaussianity of the signal can show up. This leads to larger K_n for larger smoothing scales for case A. On the other hand, smoothing decreases the non-Gaussianity of the signal. So for the noise-free case in paper I, K_n decreases with the smoothing scale. Case B has a noise level between case A and the noise-free case. The two effects of smoothing compete and cause $K_{4,5,6}$ to increase with the smoothing scale first and then decrease

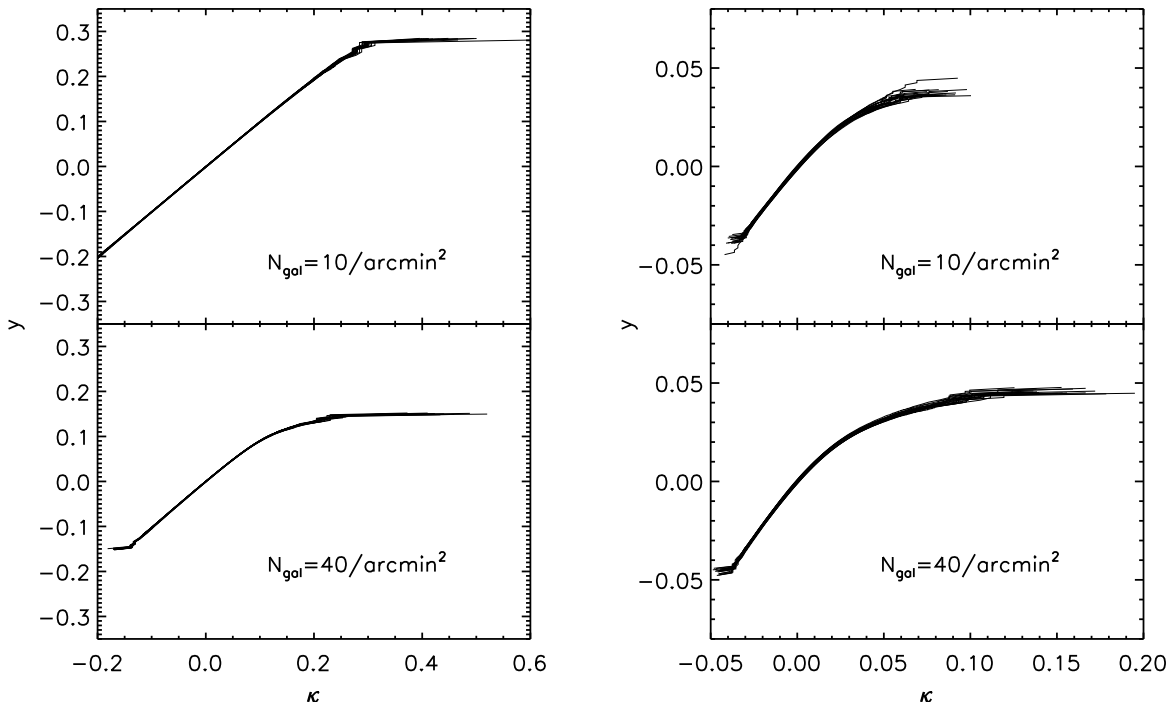


FIG. 2: The left panel shows the Gaussian transformation from noisy κ to y field, for 20 realizations. The right panel shows the result after the noise is reduced by the Wiener filter. The heavy noise make the Gaussian transformations be trivial transformation (straight line). Only few pixels survive in case A. For the noise reduced case, we can see the effect of the Wiener filter from the shape of the Gaussian transformation. The 20 Gaussian transformations converge with each other for noisy maps, and are in reasonable agreement with each other for noise reduced case. The small divergence in the latter case rises from the different normalization factors determined at zero point. Nevertheless, the normalization factor will not influence the non-Gaussianity measures.

with it.

The heavy shape measurement noise contamination significantly degrades the performance of Gaussianization. For a shallower lensing survey like DES (case A), the Gaussianization has very limited capability to reduce non-Gaussianity (Fig.3, 4 & 7). As we expect, the Gaussianization works better for cases of lower noise. But even for deep surveys like LSST (case B), the Gaussianization can only moderately suppress the non-Gaussianity. It suppresses the skewness by a factor less than 2. Although the situation is better for higher-order cumulants, the suppression factor is still less than 10 for $K_{4,5,6}$.

C. The bispectrum of noisy maps

Another measure of non-Gaussianity is the reduced bispectrum $q(\vec{l}_1, \vec{l}_2, \vec{l}_3) \equiv q(\ell, u, \alpha)$, which vanishes for Gaussian fields. The reduced bispectrum for various configurations are presented in Fig.8. Gaussianization virtually fails to reduce the bispectrum for case A in which shape measurement noise dominates. So we only show the results for case B. To better demonstrate the impact of shape noise, we choose the same 9 configurations of

$l \in [200, 6000)$ as in paper I. For most configurations of (l, u, α) , q can only be suppressed by the Gaussianization by a small factor. For many configurations, the qs after the Gaussianization deviate significantly from zero, and keep positive. This result differs from the noise-free case in paper I, in which the qs are consistent with and scatter about zero. Since the bispectrum is a measure of nonlocal pixel correlation, these results show the failure of the Gaussianization. This poor performance of the Gaussianization is consistent with the results in the previous section on the skewness, which is the bispectrum weighted over all configurations.

IV. GAUSSIANIZATION PERFORMANCE ON WIENER FILTERED MAPS

The way that Gaussianization works is that it relatively down weights large κ pixels (regions) which are mostly responsible for the non-Gaussianity. Hence to improve the performance of Gaussianization for noisy lensing maps, we shall apply a filter to down weight the noise where the signal is large. In this way the power of Gaussianization can still persist. The Wiener filter has the

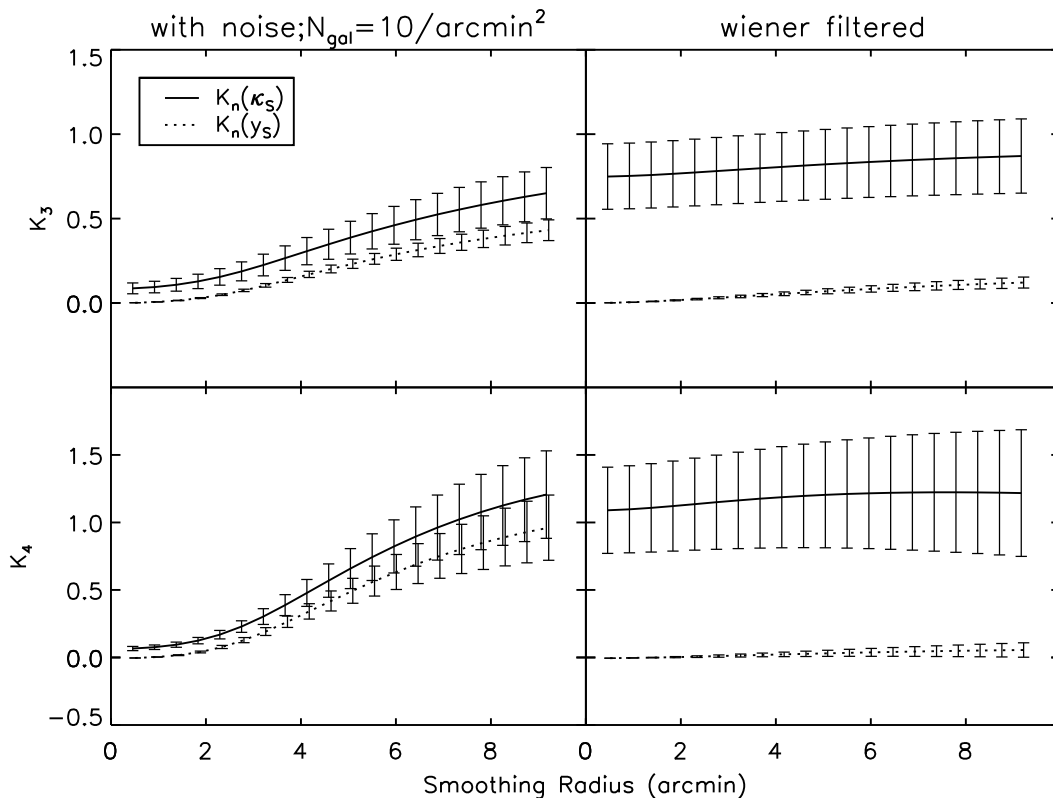


FIG. 3: The skewness (top) and kurtosis (bottom) of the smoothed noisy (left) and noise reduced (right) convergence maps are plotted in solid line, as a function of smoothing scale for case A. The results of the Gaussianized fields are plotted in dotted line. The errors are estimated from 20 realizations. The Gaussianization cannot reduce the skewness and kurtosis of these noisy maps to acceptable level. When the noise is reduced by the Wiener filter, the Gaussianization suppress the skewness and kurtosis well towards zero for all smoothing scale we considered.

desirable property. It is also widely used in astronomy. In particular, it is shown by [11] that the Wiener filter can improve the reconstruction of one-point (true) convergence PDF from noisy lensing maps.

A. The Wiener filter

In signal processing, Wiener filter is widely used to reduce the amount of noise present in a signal by comparison with an estimation of the desired noiseless signal. For simplicity, we briefly review the Wiener filter in 1D space. Assumed that the corrupted signal is $\hat{s}(x) = s(x) + n(x)$, in which $s(x)$ is the original signal and $n(x)$ is the noise. We can convolve \hat{s} with a filter $h(x)$ to reconstruct the signal s . The reconstruction error has a dispersion

$$E(H(k)) = \int dk |H(k)[S(k) + N(k)] - S(k)|^2 \quad (5)$$

in which $H(k)$, $S(k)$, $N(k)$ are the Fourier transforms of $h(x)$, $s(x)$ and $n(x)$ respectively. The Wiener filter is the one to minimize E ,

$$H(k) = \frac{|S(k)|^2}{|S(k)|^2 + |N(k)|^2}. \quad (6)$$

At scales where the signal dominate over the noise, the filter is close to 1, while at scales where the noise dominate over the signal, the filter is close to 0. This is a desirable property for our purpose.

In our application, the $|S(k)|^2$ term in the Wiener filter is the power spectrum of κ field $P(\ell) = \langle |\kappa(\vec{\ell})|^2 \rangle$. The $|N(k)|^2$ term is the Gaussian white shape noise power spectrum, which does not vary with scale.

We will basically redo the analysis in Sec.III, for noise reduced maps by the Wiener filter Eq.6.

The PDFs of Wiener filtered convergence maps are presented in the right panel of Fig.1. Compared to the unfiltered maps in the left panel, Wiener filter indeed recovers the lensing signal to some extent and as a consequence, the PDFs are now visibly non-Gaussian, even for case A which has larger measurement noise. Nevertheless, the Wiener filter significantly improve the PDF recovery. Later we will show that the gain of non-Gaussianity of the maps. But compared to the strong non-Gaussianity existed in the noise-free case, it is obvious that the Wiener filter can not recover the field too much. For case A, the PDF is still close to Gaussian distribution. The recovery effect is more obvious for case B.

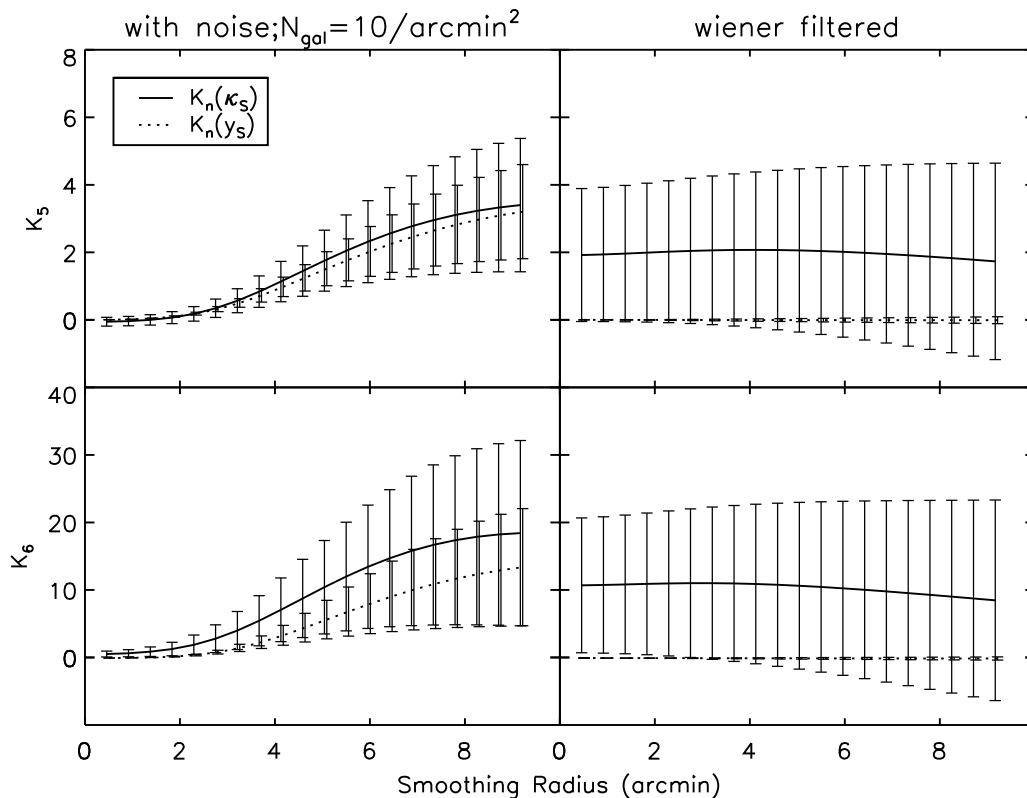


FIG. 4: The 5th- (top) and 6th- (bottom) order cumulants of the smoothed noisy (left) and noise reduced (right) convergence maps are plotted in solid line, as a function of smoothing scale for case A. The results of the Gaussianized fields are plotted in dotted line. The errors are estimated from 20 realizations. The Gaussianization cannot reduce 5th- and 6th-order cumulants of these noisy maps to acceptable level. When the noise is reduced by the Wiener filter, the Gaussianization suppress 5th- and 6th-order cumulants well to zero for all smoothing scale we considered.

B. The κ - y relation of noise reduced maps

The Gaussian transformations for the noise reduced convergence maps are presented in the right panel of Fig.2. Compared to the left panel, the shape of the transformation $\kappa \rightarrow y$ apparently changes. The turning points between the straight line $y = \kappa$, which present the domination of Gaussian noise, and the high κ end, where the Gaussianization takes effect, shift towards low κ value. Though heavy noise still makes the Gaussian transformations be a trivial mapping for the low κ value pixels, more high κ value pixels outstand the noise, and thus the Gaussianization method will have effects on these high κ value pixels. The 20 Gaussian transformations after noise reduction are in reasonable agreement with each other for both case A and B, except for one realization in case A, which have a larger normalization factor than the others. We argue that this rise from the error in normalization determined at zero point of κ . Nevertheless, the normalization factor will not influence our measures of non-Gaussianity.

C. The cumulants of noise reduced maps

The cumulants $K_{3,4,5,6}$ for the noise reduced case are presented in the right column of Fig.3 & 4 for case A and Fig.5 & 6 for case B. The solid lines are for the filtered convergence maps prior to the Gaussianization $K_n(\kappa_S^{\text{WF}})$, while the dotted lines for afterwards $K_n(y_S^{\text{WF}})$, in which superscript WF means that the noise is reduced by Wiener filter. All the results are averaged over 20 realizations and the errors are estimated. The ratio of the cumulants $K_n(y_S^{\text{WF}})/K_n(\kappa_S^{\text{WF}})$ are presented in the right column of Fig.7.

The maps with noise reduction have more skewness than the case without noise reduction (left column), and have less skewness than the noise-free case in the former work, which is just as we can expect from the PDF result. On large smoothing scales, the recovery of the non-Gaussianity due to the smoothing out of the noise and the reduction of the non-Gaussianity due to the smoothing of the signal seems to just cancel each other for case A, leading to approximately constant skewness. Similar results also occurs for $K_{4,5,6}$. Also, in case B, for $K_{4,5,6}$ on large smoothing scales, the reduction effect dominate over the recovery effect. We can see the cumulants keep

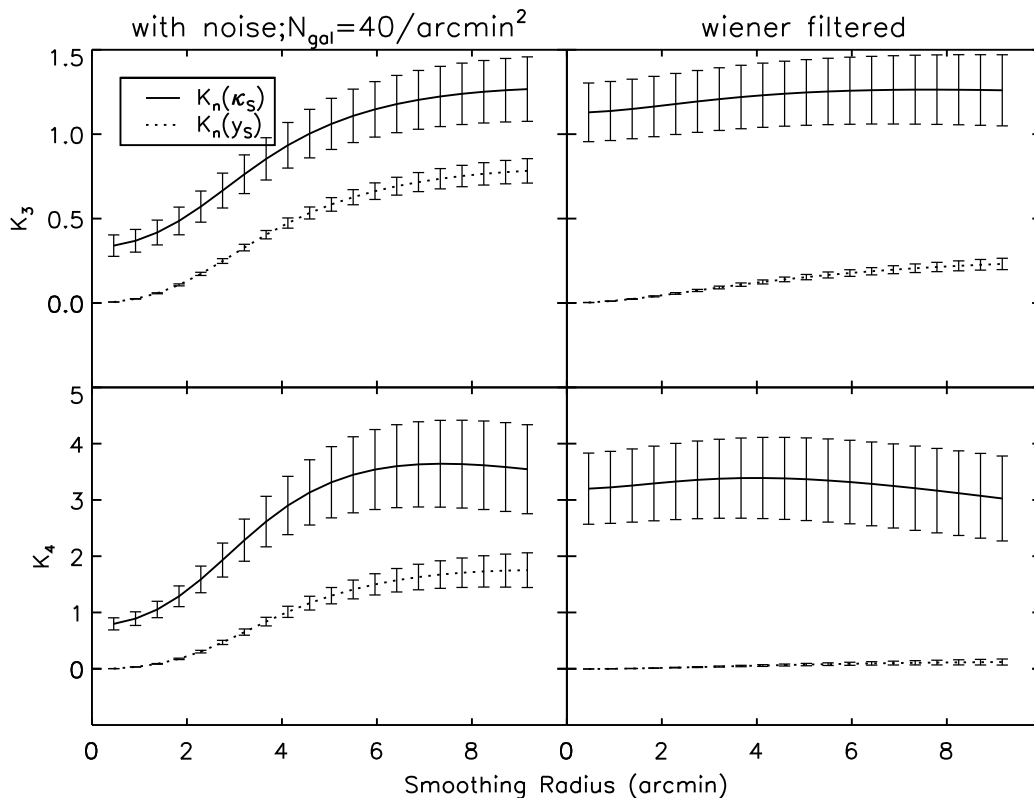


FIG. 5: The skewness (top) and kurtosis (bottom) of the smoothed noisy (left) and noise reduced (right) convergence maps are plotted in solid line, as a function of smoothing scale for case B. The results of the Gaussianized fields are plotted in dotted line. The errors are estimated from 20 realizations. The Gaussianization cannot reduce the skewness and kurtosis of these noisy maps to acceptable level. When the noise is reduced by the Wiener filter, the Gaussianization suppress kurtosis well towards zero for all smoothing scale we considered. But for the skewness, we still see remain non-Gaussianity.

constant first on small smoothing scales due to the equilibrium of the two opposite effects, and decreases on large smoothing scales due to the overwhelming reduction effect.

For both case A and B, for all order cumulants we considered, the Gaussianization works much better than the case without noise reduction. But we still see non-zero skewness on the largest smoothing scale. Kurtosis, 5th- and 6th-order cumulants of the Gaussianized maps are well consistent with zero within errors. The Gaussianization also reduce the variance among different realizations.

We can quantify the performance of the Gaussianization in the right column of Fig.7. For both case A and B, the Gaussianization can suppress the skewness a factor of 5 on the largest smoothing scale, and better (more than 10) in higher-order cumulants. The Gaussianization has much better performance on the Wiener filtered case as we expected, since the Wiener filter outstand the signal and the Gaussianization works on more pixels that dominated by non-Gaussian signal.

D. The bispectrum of noise reduced maps

The reduced bispectrum of noise reduced maps for various configurations are presented in Fig.9, where the solid lines are for the noise reduced fields κ^{WF} and dotted lines are for the corresponding y^{WF} fields. The results are averaged over the 20 realizations and the error bars are the rms dispersions within the 20 realizations. We show the bispectrum on the same 9 configurations as the qs in the last section and in the former work. For most configurations of (l, u, α) , $q(\kappa^{\text{WF}})$ s prior to the Gaussianization has larger values than the results in the previous section, due to the recovery of non-Gaussianity by the Wiener filter. We can see that after the noise reduction, qs can be significantly suppressed by the Gaussianization, and the $q(y^{\text{WF}})$ s are consistent with zero within error bars. These results show effectiveness of the Gaussianization after the noise reduction by the Wiener filter. This conclusion is consistent with the findings in the previous section on the skewness.

Since q describes the non-Gaussianity of individual configuration, to some extent it is a more sensitive measure of the performance of the Gaussianization. We find robust evidence for residual non-Gaussianity in some con-

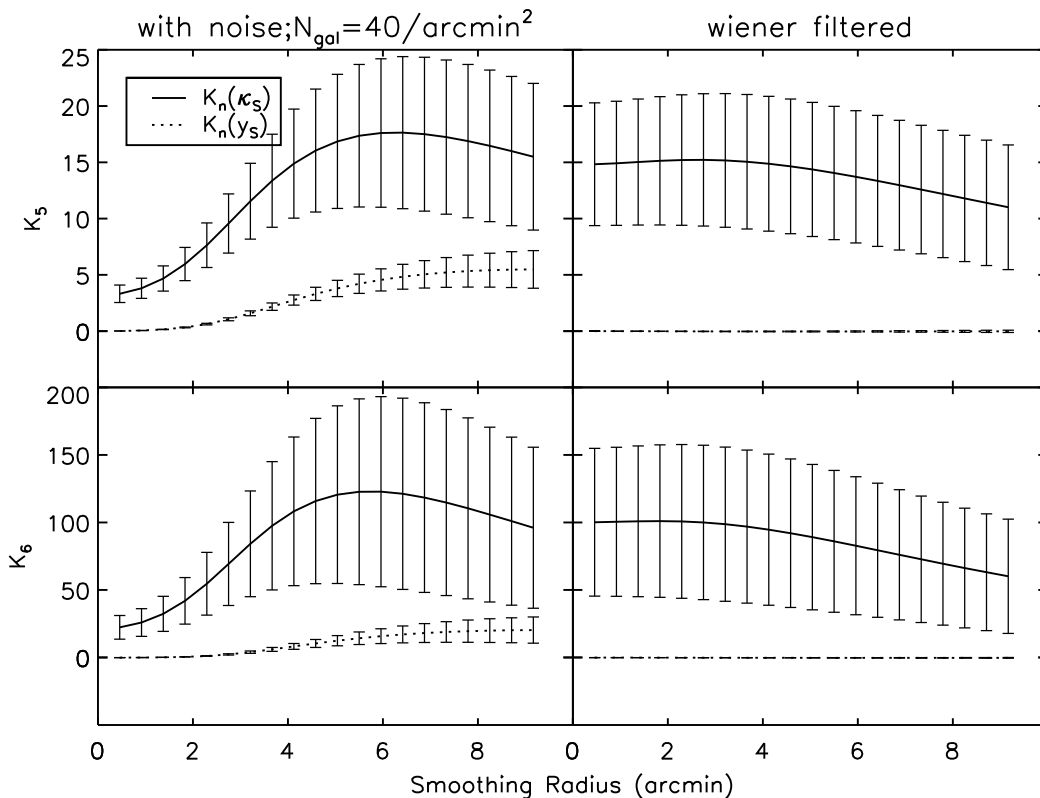


FIG. 6: The 5th- (top) and 6th- (bottom) order cumulants of the smoothed noisy (left) and noise reduced (right) convergence maps are plotted in solid line, as a function of smoothing scale for case B. The results of the Gaussianized fields are plotted in dotted line. The errors are estimated from 20 realizations. The Gaussianization cannot reduce 5th- and 6th-order cumulants of these noisy maps to acceptable level. When the noise is reduced by the Wiener filter, the Gaussianization suppress 5th- and 6th-order cumulants well to zero for all smoothing scale we considered.

figurations of the bispectrum (e.g. some configurations with large α in Fig. 9). This means that the non-Gaussianity and nonlocal pixel correlation is also not completely removed by the Gaussianization, same as the situation in the former work. A direct implication is that the Wiener filter can not fully recover the copula of the convergence field. Another source is the small deviation from Gaussian copula of the noise-free convergence field as we found in paper I [1].

V. DISCUSSIONS AND CONCLUSIONS

We have demonstrated that the Gaussianization method we proposed in the former work fails when Gaussian shape noise is added into the convergence maps. We quantify the performance of the Gaussianization by various measures of the non-Gaussianity, such as skewness, kurtosis, 5th- and 6th-order cumulants of the smoothed fields, and the bispectrum. We found that the Gaussianization can only suppress the skewness by a factor less than 2, and more or less for higher-order cumulants for different noise levels. This implies that we can not treat the resulting y field as Gaussian. There are still large

amount of information contained in high order statistics, due to the noise corruption.

We propose Wiener filter to improve the performance of the Gaussianization for the real noise existing case. We found that the noise is reduced and non-Gaussianity is recovered by the Wiener filter to some extent. The Gaussianization works well on the Wiener filtered noisy convergence maps, which is similar to the situation in the former work. The Wiener filter cannot fully recover the signal from the noise corruption, therefore the factor of non-Gaussianity measures that the Gaussianization can suppress is less than the noise-free case. The Gaussianization procedure can transport cosmological information in higher-order statistics of the Wiener filtered noisy lensing fields into the power spectrum of y . For this reason, analyzing weak lensing statistics can be simplified.

Due to the lack of fully independent realizations, and finite box size and number of particles of the simulation, our findings are inevitably affected by numerical issues such as cosmic variance, mass and force resolution, shot noise and aliasing effect [12]. We do not expect that any of these factors will alter the major conclusion on the failure of Gaussian transformation due to the heavy noise and the success after the noise reduction by the Wiener

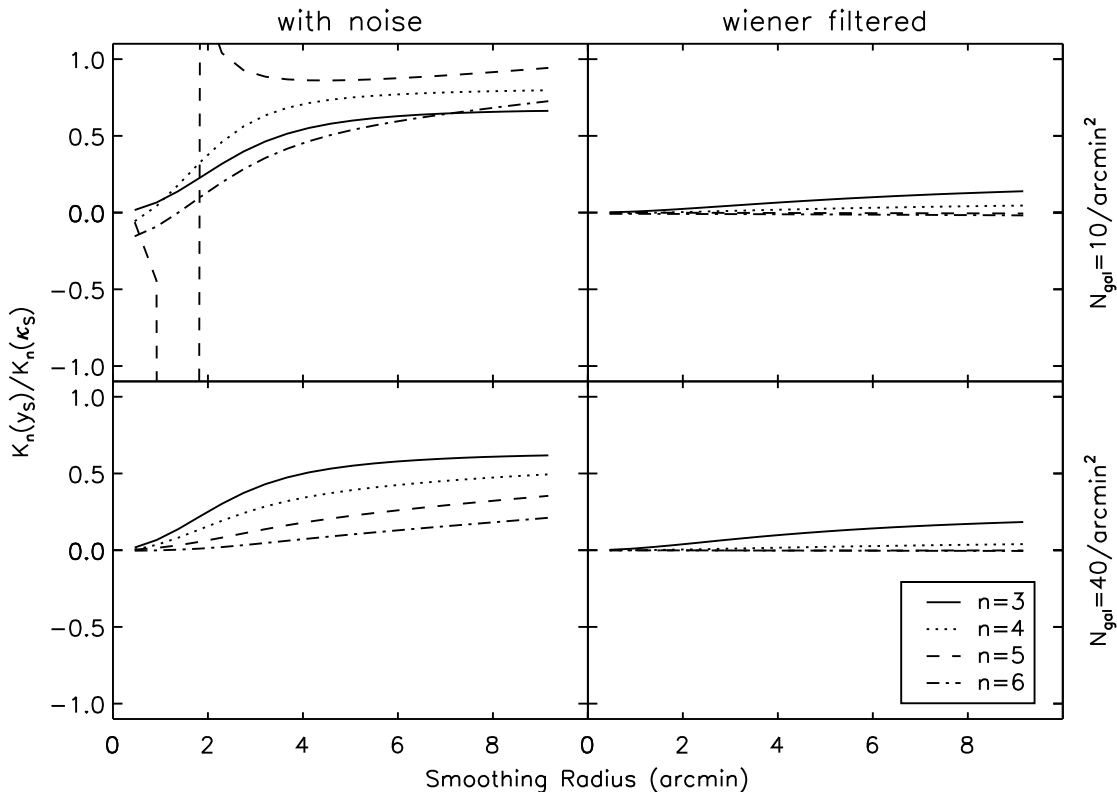


FIG. 7: The ratio of n th-order cumulants of the smoothed noisy (left) and noise reduced (right) convergence maps prior to the Gaussianization to afterwards, as a function of smoothing scale, for case A (top) and B (bottom). The Gaussianization can only suppress a factor of 2 for the skewness of a noisy map, and a little more or less for other order cumulants. When the noise is reduced by the Wiener filter, the Gaussianization suppress a factor of 5 for the skewness of a noisy map, and more than 10 for other order cumulants.

filter. These numerical issues could in particular have larger impact on the residual non-Gaussianity, which itself is weak and relatively hard to measure accurately. However, it is very unlikely that the detected residual non-Gaussianity can be canceled exactly. In this sense, the detection of the residual non-Gaussianity is robust, although we need many more simulations to measure the amplitude to high precision.

Neyrinck et al. 2010 [3] checked the effect of the logarithmic transformation and Gaussian transformation, on galaxy density field. They found that, although due to the presence of discreteness noise the galaxy density field cannot be fully Gaussianized, both transformations still dramatically reduce nonlinearities in the power spectra of cosmological matter and galaxy density fields. But the transformations do increase the effective shot noise. Neyrinck 2011 [4] studied the sensitivity of five cosmological parameters constraint to the Gaussianized power spectra by logarithmic transformation and the Gaussian transformation. He found the power spectrum of the log-density provides the tightest cosmological parameter error bars in all five parameters tested. From our studies, we found that both the noise-free case and the noisy case, the Gaussian transformation apparently devi-

ate from logarithmic transformation. Although the logarithmic transformation will not produce a perfect Gaussian random field, there is no free parameter in the transformation. Thus the information will not loss into the freedom of the transformation form, and theoretical prediction can be done, such as [13].

Joachimi et al. 2011 [5] employ an extension form of logarithmic transformation, Box-Cox transformations $\tilde{\kappa}(\lambda, a) = [(\kappa + a)^\lambda - 1]/\lambda$, with two free parameters ($\lambda \neq 0, a$) to Gaussianize ideal weak lensing convergence field. (Box-Cox transformation reduces to logarithmic transformation when $\lambda = 0$.) Optimized Box-Cox transformation is determined by fitting to Gaussian transformation through the free parameters. They developed analytical models for the transformed power spectrum, including effects of noise and smoothing and found that optimized Box-Cox transformation perform better than an offset logarithmic transformation in Gaussianizing the convergence, but none of them is capable of eliminating correlations of the power spectra between different angular frequencies. When adding a realistic level of shape noise, all the transformations perform poorly with little decorrelation of angular frequencies, and arc-tangent logarithmic transformation, which approximate a straight

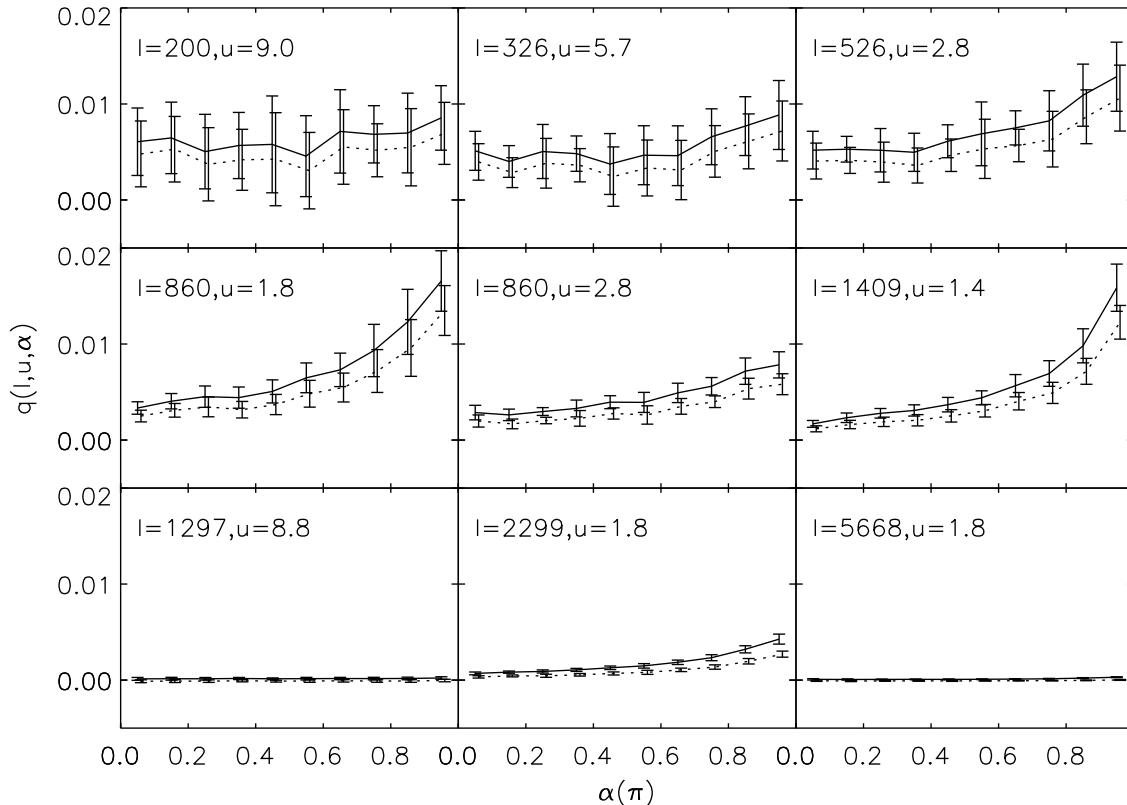


FIG. 8: The reduced bispectrum $q(\ell, u, \alpha)$ of noisy convergence maps for case B on the same 9 configurations as the previous work. The qs prior to the Gaussianization are presented in solid line, while afterwards in dotted line. The error bars are obtained from averaging over 20 respective maps. The Gaussianization can only suppress the bispectrum by a small factor, and large amount of non-Gaussianity still remains in bispectrum of the new field.

line near zero point, was proposed to deal with the shape noise situation.

There are many key issues to be explored in future study. An incomplete list includes the following.

- The applicability to real data. Although in this work we consider a more realistic case than the former work, it is still different from the real observation. The application is complicated by various measurement errors in real data. As long as the pixel size is sufficiently large, the central limit theorem drives its distribution to be Gaussian. Since the Gaussianization that we have proposed is non-linear, it will render this Gaussian noise into a non-Gaussian one. The Wiener filter could make the situation more complicate. Even worse, the same non-linear transformation and the Wiener filter could mix the lensing signal and measurement noise.
- The residual non-Gaussianity. The proposed Gaussianization works expectedly worse in noisy case and the Wiener filter works surprisingly well to deal with the noise, but it does not perfectly produce a Gaussian random field. The residual non-

Gaussianity we have detected is weak and is unlikely to carry a significant amount of cosmological information. Nevertheless, it may be still worth investigating the cosmological information carried by the residual non-Gaussianities.

- Other method dealing with noise corruption. The Gaussianization we proposed fails due to the noise corruption, and succeed in the noise-free case. The results of the Wiener filter set in somewhere between. There may exist some other appropriate tool dealing with the noise corruption and meanwhile keeps the effectiveness of the Gaussianization.

Acknowledgment

P.J.Z. thanks the support of the national science foundation of China (grant No. 10821302, 10973027 & 11025316), the CAS/SAFEA International Partnership Program for Creative Research Teams (KJCX2-YW-T23) and the 973 program grant No. 2009CB24901. W.P.L. acknowledges the supports of the Chinese National 863 project (No. 2006AA01A125), NSFC project

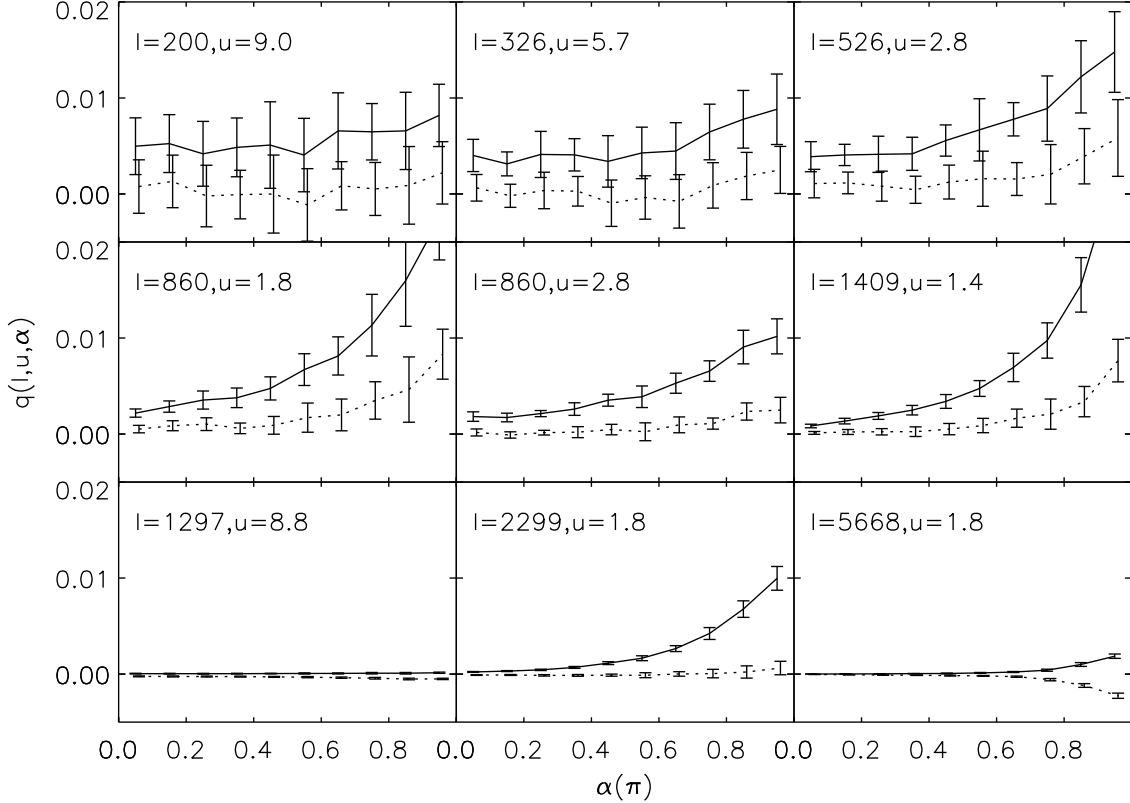


FIG. 9: The reduced bispectrum $q(\ell, u, \alpha)$ of noise reduced convergence maps for case B on the same 9 configurations. The q_s prior to the Gaussianization are presented in solid line and afterwards in dotted line. The error bars are obtained from averaging over 20 respective maps. The recovery effect of the Wiener filter result in larger value in bispectrum. The Gaussianization after noise reduction can suppress the bispectrum more, and on many configurations the bispectrum afterwards is consistent to zero within error bars. But there still exists some amount of non-Gaussianity on small scale configurations.

(10873027, 10821302), and the Knowledge Innovation Program of the Chinese Academy of Sciences (grant KJCX2-YW-T05). W.G.C. acknowledges a fellow-

ship from the European Commission's Framework Programme 7, through the Marie Curie Initial Training Network CosmoComp (PITN-GA-2009-238356).

-
- [1] Yu Yu, Pengjie Zhang, Weipeng Lin, Weiguang Cui, James N.Fry, Phys. Rev. D, 84, 023523 (2011)
- [2] Mark C. Neyrinck, Istvn Szapudi, Alexander S. Szalay, Astrophys. J. Let. 698, L90-L93 (2009)
- [3] Mark C. Neyrinck, Istvn Szapudi, Alexander S. Szalay, Astrophys. J. 731, 116 (2011)
- [4] Mark C. Neyrinck [arXiv:1105.2955]
- [5] B. Joachimi, A.N. Taylor and A. Kiessling [arXiv:1104.1399]
- [6] Hee-Jong Seo, Masanori Sato, Scott Dodelson, Bhuvnesh Jain, and Masahiro Takada, Astrophys. J. 729, L11 (2011).
- [7] Hee-Jong Seo, Masanori Sato, Masahiro Takada, Scott Dodelson [arXiv:1109.5639]
- [8] Robert J. Scherrer, Andreas A. Berlind, Qingqing Mao, Cameron K. McBride, Astrophys. J. Let. 708, L9-L13 (2010)
- [9] V. Springel. MNRAS, 364, 1105 (2005)
- [10] Weiguang Cui, Pengjie Zhang, Xiaohu Yang. PRD, 81, 103528 (2010)
- [11] Tongjie Zhang, Ue-li Pen, Astrophys. J. 635, 821 (2005)
- [12] Y.P. Jing, Astrophys. J. 620, 559 (2005)
- [13] X. Wang, M. Neyrinck, I. Szapudi, A. Szalay, X. Chen, J. Lesgourgues, A. Riotto, M. Sloth, Astrophys. J. 735, 32 (2011)
- [14] Dark Energy Survey, <http://www.darkenergysurvey.org>
- [15] <http://www.lsst.org>